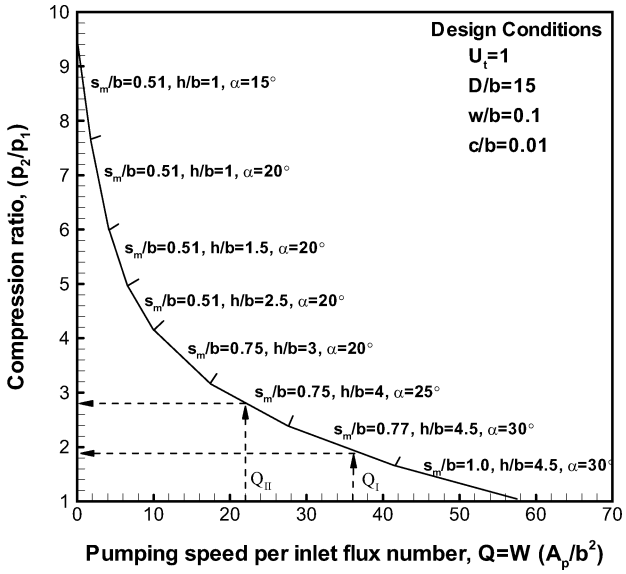

Fig. 5 The design curve for a single rotor.

Let Q_1 be the desired pumping speed at the first stage of a multirow TMP with design conditions as presented in Fig. 5. The values of compression ratio, blade angle, s_m/b, and h/b for this stage are suggested by the design curve using the following procedure. Using continuity, the pumping speed for next stage is found as $Q_1 = Q_{11}/(p_2/p_1)$ and the design curve yields the compression ratio and blade characteristics for next stage. The same steps can be used in order to find the suitable values of α, s_m/b, and h/b for next stages. As can be seen in Fig. 5, the blades of the first stages should have large angle, large heights, and great spacing-to-chord ratios, whereas for rear stages, blades with small angles, small heights, and small spacing-to-chord ratios are suitable.

Conclusions

The pumping performance of a single axial rotor in free molecular flow is investigated considering real topology of the flow passages. Good agreement between the presented method and known experimental data confirms the validity of the simulation. The parametric study for numerous sets of blade geometry yields a design curve that suggests optimum compression ratio or pumping speed for the desired conditions. The design curve shows that, for maximum pumping speed, the prior stages of a TMP should have blades with wide spacing, large height, and large angle, whereas the later stages should to be designed with small height, small angle, and small spacing.

References

[1]Kruger, C. H., and Shapiro, A. H., "The Axial-Flow Compressor in the Free-Molecule Range," *Proceedings of 2nd International Symposium on Rarefied Gas Dynamics*, Academic Press, New York, 1961, pp. 117–140.

[2]Sawada, T., Suzuki, M., and Taniguchi, O., "The Axial Flow Molecular Pump, 1st Report, on a Rotor with a Single Blade Row," Institute of Physical and Chemical Research, Japan, Vol. 62, No. 2, 1968, pp. 49–64.

[3]Katsimichas, S., Goddard, A. J. H., Lewington, R., and de Oliveira, C. R. E., "General Geometry Calculations of One-Stage Molecular Flow Transmission Probabilities for Turbomolecular Pumps," *Journal of Vacuum Science and Technology*, Vol. 13, No. 6, 1995, pp. 2954–2961.

[4]Skovorodko, P. A., "The Topology of Molecular Flow in Axial Compressor," *47th AVS International Symposium: Vacuum, Thin Films, Surfaces/Interfaces and Processing*, American Vacuum Society, New York, Oct. 2000, p. 155.

[5]Amoli, A., Hosseinalipour, S. M., and Ebrahimi, R., "Direct Simulation of Free Molecular Flow in Fully 3-D Axial Rotor," AIAA Paper 2003-3777, June 2003.

[6]Bird, G. A., *Molecular Gas Dynamics and the Direct Simulation of Gas Flows*, 2nd ed., Oxford Univ. Press, New York, 1994.

[7]Kruger, C. H., "The Axial-Flow Compressor in the Free-Molecule Range, Ph.D. Dissertation, Dept. of Mechanical Engineering, Massachusetts Inst. of Technology, Feb. 1960.

[8]Sawada, T., and Taniguchi, O., "The Axial Flow Molecular Pump, 3rd Report, Trial Manufacture and Performance Test," *Bulletin of the Japan Society of Mechanical Engineers*, Vol. 16, No. 92, 1973, pp. 312–318.

Backward Monte Carlo Method Based on Radiation Distribution Factor

L. H. Liu*
Harbin Institute of Technology,
150001 Harbin, People's Republic of China

Introduction

MONTE Carlo method simulates radiative transfer by tracing the histories of a number of rays that represent photon bundles traveling through the medium.[1,2] There are two types of Monte Carlo methods, namely, the forward Monte Carlo method and the backward (or reverse) Monte Carlo method. Forward Monte Carlo methods simulate a history of photon bundle starting at emission and ending at absorption, determining how much radiation power is transferred from one region to another. Backward Monte Carlo methods start at a termination site, for example, detector, and trace the photon bundle in the reverse direction, determining how much radiation power emitting along the path is incident on the termination site. For a measurement problem, using forward Monte Carlo simulation, one would emit and trace many photon bundles, even though only the tiniest of fraction will hit the detector. In this case, forward Monte Carlo simulation can become terribly inefficient. However, backward Monte Carlo simulation can alleviate this problem.

The backward Monte Carlo technique is based on the principle of reciprocity in radiative transfer theory as described by Case.[3] Walters and Buckius[4] developed a comprehensive reverse Monte Carlo method for computing the emission of a generalized enclosure containing an absorbing, emitting, and scattering medium. Modest[5] gave a comprehensive formulation for backward Monte Carlo simulation, capable of treat emitting, absorbing, and anisotropically scattering media with collimated irradiation, point, or line sources. If the temperature or the collimated irradiation are changed, even if the absorption and scattering coefficients of medium do not depend on temperature, backward Monte Carlo techniques of Walters and Buckius[4] and Modest[5] need to restart to trace all photon bundles from the beginning. Sometimes, this will suppress the efficiency of these methods, especially for inverse analysis of temperature field by using the outgoing emission intensity through a pore on the boundary of enclosure. This problem can be overcome by using the concept of radiation distribution factor[6] in the case that the radiative properties of medium and boundary do not depend on temperature.

The objective of this Note is to develop a backward Monte Carlo method based on the concept of radiation distribution factor and extend it to the cases with collimated irradiation, point, or line sources. A same example used by Modest[5] is applied to verify this new strategy.

Mathematical Formulation

As shown in Fig. 1, a three-dimensional semitransparent gray absorbing-emitting-scattering medium is bounded by connected

Received 19 May 2003; revision received 8 August 2003; accepted for publication 2 September 2003.

*Professor, School of Energy Science and Engineering, 92 West Dazhi Street; liulh_hit@263.net.

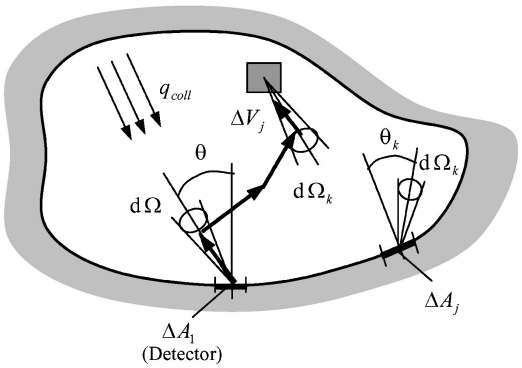

Fig. 1 Backward ray tracing in a multidimensional enclosure with an absorbing, emitting, and scattering medium.

surface. This geometrical enclosure is divided into many small surface and volume elements. Suppose that for $1 \le i \le N$ the elements are surface elements bounding the enclosure, and for $N+1 \le i \le M$ the elements are volume elements. The object is to determine the flux incident on the surface element ΔA_1 in a differential solid angle $d\Omega$ along the incidence angle θ.

From the definition of the radiation distribution factor,[6] the radiant power emitted from the surface element ΔA_1 in solid angle $d\Omega$ along the incidence angle θ and absorbed by surface elements $(1 \le j \le N)$ and volume element $(N+1 \le j \le M)$ in a differential solid angle $d\Omega_k$ can be written as

$$Q_{1^*j} = \Delta A_1 \varepsilon_1 \cos\theta \, d\Omega \, I_b(T_1) D_{1^*jk} \tag{1}$$

where ε is the emissivity, I_b is the blackbody radiative intensity, and T is the temperature. The radiation distribution factor D_{1^*jk} is defined as the fraction of the total radiation emitted from the surface element ΔA_1 in the solid angle $d\Omega$ that is absorbed by surface or volume element j in the solid angle $d\Omega_k$, as a result of both direct radiation and all possible reflection or scattering. The radiation distribution factor D_{1^*jk} can be determined via the standard or the energy partitioning ray tracing technique, that is, starting from the surface element ΔA_1, tracing the photon bundles emitted by the surface element ΔA_1 in the solid angle $d\Omega$, and determined by how much fraction of energy is absorbed by the element j in the solid angle $d\Omega_k$. Similarly, the radiant power emitted by surface or volume element j in a differential solid angle $d\Omega_k$ and absorbed by the surface element ΔA_1 in solid angle $d\Omega$ along the angle θ can be written as

$$Q_{j1^*} = \Delta A_j \varepsilon_j \cos\theta_k \, d\Omega_k \, I_b(T_j) D_{j1^*}, \qquad 1 \le j \le N \tag{2}$$

$$Q_{j1^*} = \kappa_j \, d\Omega_k \Delta V_j I_b(T_j) D_{j1^*}, \qquad N+1 \le j \le M \tag{3}$$

where κ is the absorption coefficient and ΔA and ΔV are the area of surface and the volume of volume element, respectively. The radiation distribution factor D_{jk1^*} is defined as the fraction of the total radiation emitted from surface or volume element j that emerges into the surface element ΔA_1 in solid angle $d\Omega$ along the angle θ.

According to the reciprocity of radiation distribution factor, we have

$$\Delta A_1 \varepsilon_1 \cos\theta \, d\Omega D_{1^*jk} = \Delta A_j \varepsilon_j \cos\theta_k \, d\Omega_k D_{jk1^*} \qquad 1 \le j \le N \tag{4}$$

$$\Delta A_1 \varepsilon_1 \cos\theta \, d\Omega D_{1^*jk} = \kappa_j d\Omega_k \Delta V_j D_{jk1^*} \qquad N+1 \le j \le M \tag{5}$$

After D_{1^*jk} or D_{jk1^*} have been solved, the radiant heat absorbed by the surface element ΔA_1 in solid angle $d\Omega$ can be calculated by Eqs. (1–5). For forward Monte Carlo simulation, radiant energy emerging from the enclosure system and emitting into the surface element ΔA_1 in solid angle $d\Omega$ along the angle θ is given by

$$Q_{1^*} = \sum_{j=1}^{N} \sum_{k} \Delta A_j \cos\theta_k \, d\Omega_k D_{jk1^*} \varepsilon_j I_b(T_j) + \sum_{j=N+1}^{M} \sum_{k} d\Omega_k \, \Delta V_j \, D_{jk1^*} \kappa_j I_b(T_j) \tag{6}$$

For backward Monte Carlo simulation, Q_{1^*} is computed by

$$Q_{1^*} = \sum_{j=1}^{M} \sum_{k} \Delta A_1 \varepsilon_1 \cos\theta \, d\Omega \, D_{1^*jk} I_b(T_j) \tag{7}$$

In backward Monte Carlo simulation, only the radiant energy emitting from the surface element ΔA_1 in solid angle $d\Omega$ is traced, whereas in forward Monte Carlo simulation the radiant energy emitted from all of the volume element and the surface element needs to be traced. On the other hand, a very small part of the energy bundles emitted from each surface or volume element can enter into the differential solid angle $d\Omega$. This results in the slow convergence of forward Monte Carlo simulation.

For collimated irradiation, radiation energy can be separated into a direct (collimated) and a diffuse part [first scattering and reflection, see Eqs. (18.12–18.15) in Ref. 2]. If the scattering is anisotropic and the boundary is diffuse, the source terms $\varepsilon_j I_b(T_j)$ and $\kappa_j I_b(T_j)$ in Eq. (6) need to be replaced by $\varepsilon_j I_b(T_j) + I^r_{djk}$ and $\kappa_j I_b(T_j) + I^s_{djk}$, respectively. For forward Monte Carlo simulation, in the case of collimated irradiation the radiant energy emerging from the enclosure system and emitting into the surface element ΔA_1 in solid angle $d\Omega$ along the angle θ is given by

$$Q_{1^*} = \Delta A_1 \varepsilon_1 q_{\text{direct}} + \sum_{j=1}^{N} \sum_{k} \Delta A_j \cos\theta_k \, d\Omega_k D_{jk1^*} \times \left[\varepsilon_j I_b(T_j) + I^r_{djk}\right] + \sum_{j=N+1}^{M} \sum_{k} d\Omega_k \Delta V_j \, D_{jk1^*} \times \left[\kappa_j I_b(T_j) + I^s_{djk}\right] \tag{8}$$

where

$$I^r_{djk} = (1-\varepsilon_j) \frac{q_{\text{coll}}(r_w)}{\pi} \exp\left[-\int_0^{l_c} (\kappa+\sigma_s) \, dl\right] \qquad 1 \le j \le N \tag{9}$$

$$I^s_{djk} = \sigma_{sj} \frac{q_{\text{coll}}(r_w)}{4\pi} \exp\left[-\int_0^{l_c} (\kappa+\sigma_s) \, dl\right] \Phi(\mathbf{s}_0, \mathbf{s}_k) \qquad N+1 \le j \le M \tag{10}$$

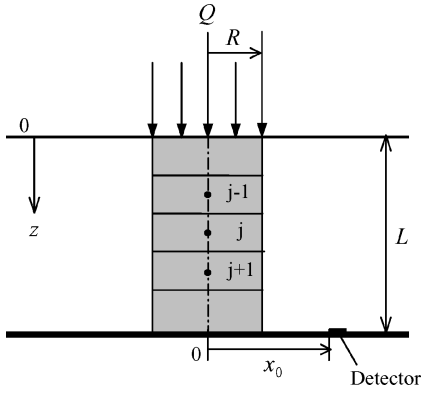

Fig. 2 One-dimensional slab with normally incident collimated irradiation.

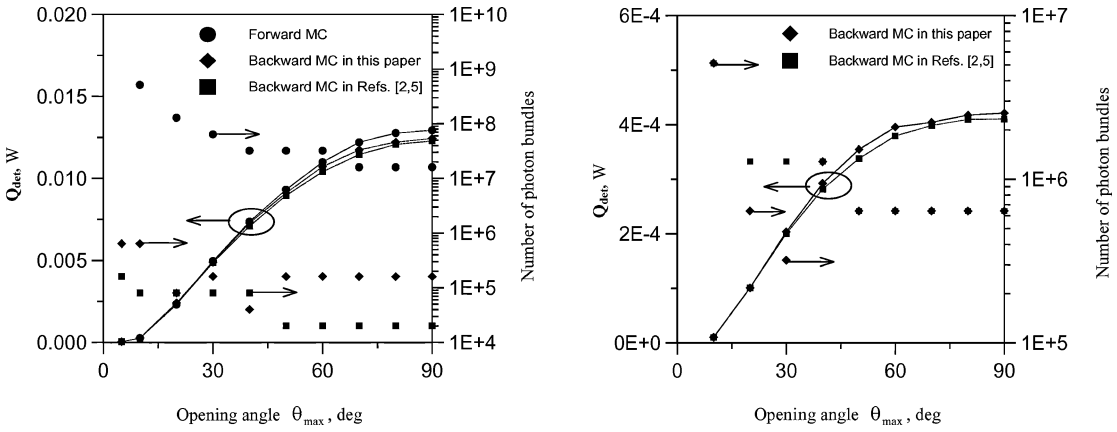

Fig. 3 Detector fluxes and required number of photon bundles: a) $\sigma_s = 1\ \mathrm{m}^{-1}$, $\kappa = 1\ \mathrm{m}^{-1}$, and $\Phi = 1$; and b) $\sigma_s = 1\ \mathrm{m}^{-1}$, $\kappa = 5\ \mathrm{m}^{-1}$, and $\Phi = 1 + 2\cos\theta$.

Here, q_{coll} is the collimated flux entering medium, σ_s is the scattering coefficient, Φ is the single scattering phase function, q_{direct} is the collimated flux incident on the surface element ΔA_1 in solid angle $\mathrm{d}\Omega$, I^s_{djk} and I^r_{djk} denote the additional source terms caused by the first scattering and the first reflection of the collimated irradiation, respectively, and l_c is the traveling distance of collimated irradiation. If the collimated irradiation does not pass through or hit the surface or volume element j, $I^r_{djk} = 0$, or $I^s_{djk} = 0$.

From Eq. (8), by using the reciprocity of radiation distribution factor [see Eqs. (4) and (5) we can obtain the corresponding formula for the backward Monte Carlo simulation:

$$Q_{1^*} = \Delta A_1 \varepsilon_1 q_{\mathrm{direct}} + \sum_{j=1}^{N} \sum_{k} \Delta A_1 \varepsilon_1 \cos\theta \, \mathrm{d}\Omega \, D_{1^* jk} \times \left[I_b(T_j) + \frac{I^r_{djk}}{\varepsilon_j} \right] + \sum_{j=N+1}^{M} \sum_{k} \Delta A_1 \varepsilon_1 \cos\theta \, \mathrm{d}\Omega D_{1^* jk} \times \left[I_b(T_j) + \frac{I^s_{djk}}{\kappa_j} \right] \tag{11}$$

Results and Discussions

For the sake of comparison, we consider a same example used by Modest,[5] in which a one-dimensional slab $0 < z \le 1 = 1$ m of a gray, absorbing, scattering cold medium, is bounded at the top by vacuum and at the bottom by a cold, black surface. Collimated irradiation of strength $Q = 100$ W is normally incident on this nonreflecting layer, equally distributed over the disk $0 \le r \le R = 0.1$ m. A small detector 5×5 cm in size, with an acceptance angle of $\theta_{\max}$, is located on the black surface at $x = x_0 = 0.2$ m, $y = 0$. The object is to determine the flux Q_{det} incident on the detector within varying acceptance angles. As shown in Fig. 2, the irradiated zone is divided into 100 sublayers. The 4π solid angle is divided into 40 uniform parts. Using the previously developed backward Monte Carlo method based on radiation distribution factor, Q_{det} can be written as

$$Q_{\mathrm{det}} = \Delta A\left(1 - \cos^2\theta_{\max}\right) \sum_{j} \sum_{k} \frac{D_{1^* jk}}{4\pi R^2 \kappa_j} \sigma_s Q \times \exp[-(\kappa + \sigma_s) z_j] \Phi(\boldsymbol{s}_0, \boldsymbol{s}_k) \tag{12}$$

Results are shown in Fig. 3 and compared with those of the forward and the backward Monte Carlo methods developed by Modest,[5] in which the computer programs (fwdmcck1 and revmcck1) in Appendix F of Ref. 2 are used for the case of isotropic scattering and extended for the case of linear anisotropic scattering. Fig. 3a shows the results for the case of isotropic scattering, and Fig. 3b shows the results for the case of anisotropic scattering. Here, in all simulations the standard ray tracing[2] was used, and the number of photon bundles was doubled again and again until a relative standard deviation of less than 2% of the desired quantity was achieved. From Fig. 3, it can be seen that the results agree with each other, but the number of required photon bundles to achieve a given standard deviation is different. The number of required photon bundles for the forward Monte Carlo simulation is much larger than that of the backward Monte Carlo simulation. In general, the number of required photon bundles for the backward Monte Carlo method based on radiation distribution factor is in the same order as that for the backward Monte Carlo method developed by Modest.[5]

Conclusions

A backward Monte Carlo method based on the concept of radiation distribution factor has been developed and extended to the cases with collimated irradiation. An example is applied to verify this new strategy and compared with other backward Monte Carlo strategies. The efficiency of the backward Monte Carlo method based on the concept of radiation distribution factor is same as the backward Monte Carlo strategy developed by Modest. If the temperature or the collimated irradiation are changed and the absorption and scattering coefficients of medium do not depend on temperature, the backward Monte Carlo strategy developed in this paper will be more efficient than others. However, because the concept of radiation distribution factor is based on the absorption distribution of radiation energy this method cannot be used in the case of pure scattering problems with collimated irradiation.

References

[1] Siegel, R., and Howell, J. R., *Thermal Radiation Heat Transfer*, 3rd ed., Taylor and Francis, Washington, DC, 1992, pp. 795–804.

[2] Modest, M. F., *Radiative Heat Transfer*, 2nd ed., Academic Press, San Diego, CA, 2003, pp. 644–676, 787.

[3] Case, K. M., "Transfer Problems and the Reciprocity Principle," *Review of Modern Physics*, Vol. 29, No. 4, 1957, pp. 651–663.

[4] Walters, D. V., and Buckius, R. O., "Rigorous Development for Radiation Heat Transfer in Nonhomogeneous Absorbing, Emitting and Scattering Media," *International Journal of Heat and Mass Transfer*, Vol. 35, No. 12, 1992, pp. 3323–3333.

[5] Modest, M. F., "Backward Monte Carlo Simulations in Radiative Heat Transfer," *Journal of Heat Transfer*, Vol. 125, No. 1, 2003, pp. 57–62.

[6] Mahan, J. R., *Radiation Heat Transfer*, Wiley, New York, 2002, pp. 390–408.